

# Glass–liquid transition of water at high pressure

Ove Andersson<sup>1</sup>

Department of Physics, Umeå University, 901 87 Umeå, Sweden

Edited by H. Eugene Stanley, Boston University, Boston, MA, and approved May 25, 2011 (received for review November 8, 2010)

The knowledge of the existence of liquid water under extreme conditions and its concomitant properties are important in many fields of science. Glassy water has previously been prepared by hyperquenching micron-sized droplets of liquid water and vapor deposition on a cold substrate (ASW), and its transformation to an ultraviscous liquid form has been reported on heating. A densified amorphous solid form of water, high-density amorphous ice (HDA), has also been made by collapsing the structure of ice at pressures above 1 GPa and temperatures below approximately 140 K, but a corresponding liquid phase has not been detected. Here we report results of heat capacity  $C_p$  and thermal conductivity, in situ, measurements, which are consistent with a reversible transition from annealed HDA to ultraviscous high-density liquid water at 1 GPa and 140 K. On heating of HDA, the  $C_p$  increases abruptly by  $(3.4 \pm 0.2) \text{ J mol}^{-1} \text{ K}^{-1}$  before crystallization starts at  $(153 \pm 1) \text{ K}$ . This is larger than the  $C_p$  rise at the glass to liquid transition of annealed ASW at 1 atm, which suggests the existence of liquid water under these extreme conditions.

glass transition | pressure-induced amorphization | relaxation

Unlike most liquids that vitrify by normal supercooling, water vitrifies only by hyperquenching of its micron-size droplets, and its porous amorphous state is made by vapor deposition (1–3). Pure bulk water densified by high pressure also does not vitrify on normal cooling; instead it freezes to proton-disordered high-density ices. However, in 1984 Mishima et al. (4) discovered a path to obtain a high-density amorphous ice (HDA) by pressurization of hexagonal ice, ice Ih, to approximately 1.5 GPa at 77 K. This amorphous form is characterized by the absence of Bragg peaks, but it is heterogeneous on a mesoscopic length scale (5). On heating at high pressures above approximately 0.5 GPa (6), it relaxes, homogenizes, and densifies before crystallization, and the ultimately densified form has been referred to as very high-density amorphous ice (vHDA) (7). There are thus a multiplicity of amorphous states with densities in between HDA and vHDA, which are produced by isothermal pressurization of ice Ih at temperatures below approximately 140 K, and these are here generically referred to as HDA.

States of water at extreme pressure and temperature conditions are important for, for example, understanding of tectonics in large bodies of the outer solar system where ice is one of the rock-forming minerals (8), and for water's phase diagram and properties (9), but it is not known whether HDA transforms to glassy and liquid states on heating. This work reports a unique high-pressure, in situ, heat capacity  $C_p$  study of HDA just below its crystallization point where a glass to liquid transition may occur. It is here shown that HDA exhibits a glass transition with a heat capacity rise larger than that for amorphous solid water and hyperquenched water at 1 atm, which suggests a thermodynamic path between the annealed state of HDA and liquid water. The glass transition at 1 GPa is observed as a sigmoid shape change in  $C_p$  and a peak in thermal conductivity for a time scale of approximately 1 s at 140 K.

## Results and Discussion

Measurements were performed in situ by using the transient hot-wire method (see *Materials and Methods* and *SI Text*) that allowed for simultaneous measurement of heat capacity per unit

volume,  $c$ , (or the product of the specific heat capacity and density), and thermal conductivity  $\kappa$ . About 17 mL of pure water was frozen in a Teflon cell (Fig. S1) placed inside a high-pressure vessel, and the pressure raised to approximately 0.05 GPa. The sample was cooled to approximately 100 K, reheated and stabilized before it was pressurized isothermally at  $(129 \pm 1) \text{ K}$  to 1.25 GPa at  $0.1 \text{ GPa h}^{-1}$  rate to collapse ice Ih to HDA. The results on cooling at 0.05 GPa agreed to within 2% with literature values (Fig. S2).

Fig. 1A shows that  $c$  of ice at 129 K gradually decreases linearly on pressurizing up to 0.7 GPa. This is the region in which ice lattice elastically deforms and the volume decreases while the phonon frequency increases, as generally observed for materials. The latter decreases  $c$  whereas the reduced volume increases  $c$ . On compression of ice up to a pressure of 0.7 GPa, the slowly decreasing  $c$  is due to the effect of pressure predominantly on the phonon frequency. On further compression,  $c$  rapidly decreases and reaches a local minimum at 0.84 GPa. As collapse of the ice structure begins, the initial increase in density decreases  $c$  rapidly as a premonitory occurrence to its full collapse, after which decompression does not restore the original structure of ice. Neutron scattering studies (10) have shown that as structural collapse occurs, extra  $\text{H}_2\text{O}$  molecules are forced to move into the first coordination shell of the hydrogen bonded four near neighbors of a reference  $\text{H}_2\text{O}$  molecule. The density increases initially gradually, but the phonon frequency increases much more rapidly. The overwhelming effect of the latter causes  $c$  to decrease rapidly. In the pressure range 0.85–1.0 GPa, the structure strongly densifies as the extra  $\text{H}_2\text{O}$  molecules enter their (interstitial) sites in first coordination shell.\* The resulting large and irreversible increase in density dominates, and  $c$  increases rapidly as the structure ultimately collapses with increasing pressure to HDA, which has a structure similar to that of high-density liquid water (10, 11). On further compression, the collapsed structure homogenizes with a likely overall increase in the diffusion time. The consequence of such an increase near a glass transition would be an irreversible decrease of  $c$ , like that observed here in the 1 to approximately 1.15 GPa range, until the homogenization approaches completion (see also *SI Text*). In this process, the orientationally disordered structure of ice (12) converts to a canonically disordered structure of hydrogen-bonded and interstitial  $\text{H}_2\text{O}$  molecules (i.e., a state with no long-range translational periodicity) that transforms ultimately to a kinetically frozen state, as measured on a 1 s time scale (see *Materials and Methods* and *SI Text*). Because of the heterogeneous character of the state initially formed at 1.2 GPa (5) and its subsequent further relaxation and homogenization during heating, it appears similar to the high-

Author contributions: O.A. designed research, performed research, analyzed data, and wrote the paper.

The author declares no conflict of interest.

This article is a PNAS Direct Submission.

\*Neutron diffraction data for samples recovered at 1 atm and 77 K suggest that there are approximately two interstitial  $\text{H}_2\text{O}$  molecule in vHDA, and one in HDA produced at 77 K (10).

<sup>1</sup>To whom correspondence should be addressed. E-mail: ove.andersson@physics.umu.se.

This article contains supporting information online at [www.pnas.org/lookup/suppl/doi:10.1073/pnas.1016520108/-DCSupplemental](http://www.pnas.org/lookup/suppl/doi:10.1073/pnas.1016520108/-DCSupplemental).

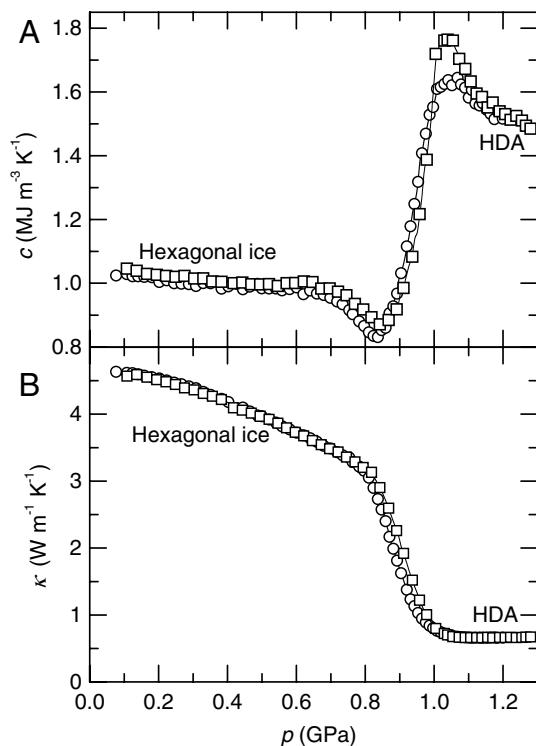


**Fig. 1.** Thermal properties prior, during, and after pressure collapse of hexagonal ice, ice Ih. (A) Heat capacity per unit volume and (B) thermal conductivity on isothermal pressurization at  $(129 \pm 1)$  K. The squares and circles show results for two different runs, which agree to within 2% outside the collapse range.

energy state of a collapsed crystal obtained by mechanical deformation (13).

Fig. 1B shows the concurrent change in  $\kappa$  on pressurizing ice at 129 K. The  $\kappa$  decreases linearly with increasing pressure until approximately 0.75 GPa, and then more abruptly in the pressure range of 0.8–1 GPa. The latter decrease is due to the structural collapse of ice that decreases the mean free path for propagation of phonons,  $l$ . This decrease dominates the changes in the parameters of the Debye's approximate relation (14),  $\kappa = cvl/3$  where  $v$  and  $c$  are the velocity and heat capacity per unit volume of the heat-carrying phonons. After a sigmoid shape decrease,  $\kappa$  reaches a plateau like value of  $0.66 \text{ W m}^{-1} \text{ K}^{-1}$  at approximately 1.15 GPa, thereby indicating that the structural collapse of ice is approaching completion.

The sample was then heated from 100 K to 148 K at  $0.4 \text{ K min}^{-1}$  rate and subsequently cooled to 100 K at  $0.3 \text{ K min}^{-1}$  at 1 GPa before reheating. On first heating of the collapsed state at 1 GPa,  $\kappa$  increases in a broad sigmoid shape manner (Fig. 2B), as the state relaxes to a lower energy and the structure densifies. On cooling from 148 K, the slope becomes negative and a peak appears at 140 K. On subsequent heating,  $\kappa$  retraces its path and a peak reappears at 140 K. This shows that the results become reversible after the first heating to 148 K, which yields the state referred to as vHDA (7). Moreover, the peak or change in the sign of  $dk/dT$  at 140 K is typical for the onset of kinetic unfreezing on heating and of kinetic freezing on cooling. It is commonly observed at glass-liquid transitions and is generally reported for, for example, those of polymers (15). It likely occurs mainly as a result of a change in the thermal expansivity. On further heating,  $\kappa$  increases rapidly, showing that crystallization began at  $(153 \pm 1)$  K, and this exothermic process was also detected by an accelerated rate for the sample

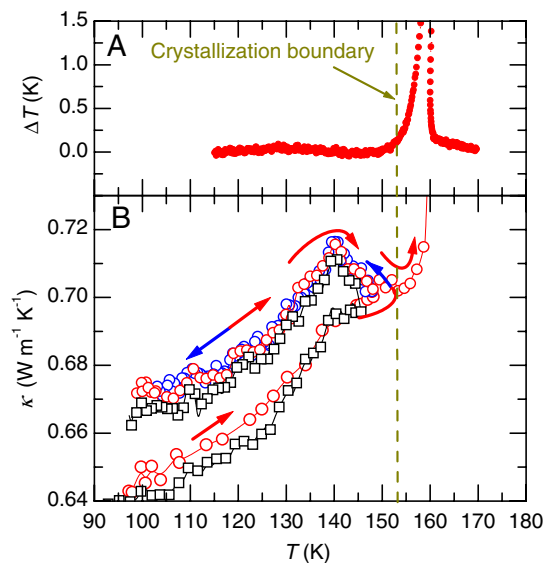


**Fig. 2.** Relaxation behavior, reversible glass transition, and crystallization. (A) Excess sample temperature, which was obtained by subtracting a function fitted to measured data for temperature vs. time below 140 K and above 165 K, during heating at 1 GPa. (B) Thermal conductivity during heating from 100 to 148 K, cooling from 148 to 100 K, and reheating to 175 K at 1 GPa. On the first heating to 148 K, the collapsed ice relaxes and apparently transforms to ultraviscous high-density liquid water at 140 K, which vitrifies on cooling. The squares and circles show results for two different runs. The increase in  $\kappa$  at approximately 153 K is due to sluggish crystallization.

temperature increase, as shown in Fig. 2A (see *SI Text* for a detailed analysis of the crystallization temperature).

In the plot of the measured  $c$  of the relaxed state at 1 GPa (second heating), shown by the circles in Fig. 3A, a sigmoid-shape increase appears with onset at 140 K. This is a characteristic feature of a glass transition that shows the temperature range of kinetic unfreezing, and from which the glass transition temperature  $T_g$  is determined. Because the density of the annealed state at 1 GPa changes by less than 1% over the temperature range of interest, the plot of  $c$  is effectively the plot of  $C_p$ , the specific heat per mole. To show the sigmoid-shape change more clearly,  $c$  in Fig. 3A was converted to  $C_p$  by using the HDA's density of  $1.35 \text{ g cm}^{-3}$  at 1.2 GPa in the 130–140 K range (16), and the difference between the measured  $C_p$  and the linearly extrapolated (vibrational)  $C_p$  from the glassy state plotted in Fig. 3B.

Fig. 3B shows that the heat capacity increase at  $T_g$  is  $(3.4 \pm 0.2) \text{ J mol}^{-1} \text{ K}^{-1}$  before the sluggish crystallization affects the results above approximately 153 K. This rise thus occurs within a temperature range of about 13 K. Although the increase tends to level off,  $C_p$  still rises when crystallization interferes with the results, which indicates that the glass transition range extends a few degrees further and that the heat capacity step is somewhat larger than  $(3.4 \pm 0.2) \text{ J mol}^{-1} \text{ K}^{-1}$ . The time scale of the method is about 1 s, which means that the (average) relaxation time of the motions associated with the glass transition is less than approximately 1 s at the onset temperature of the  $C_p$  rise. On further temperature increase, their contribution to the measured  $C_p$  increases as the relaxation time decreases. Finally, at a temperature well above  $T_g$  where the relaxation time is much less than 1 s, the increase in  $C_p$  levels off as the configurational degrees of freedom, which are frozen at  $T_g$ , equilibrate quickly. This change in the heat capacity contribution of the configurational modes can be calculated as a function of relaxation time, or temperature, by an analysis of the method. The total heat capacity step can therefore be estimated and the analysis indicates that approximately 90% of the heat capacity step has occurred when crystallization

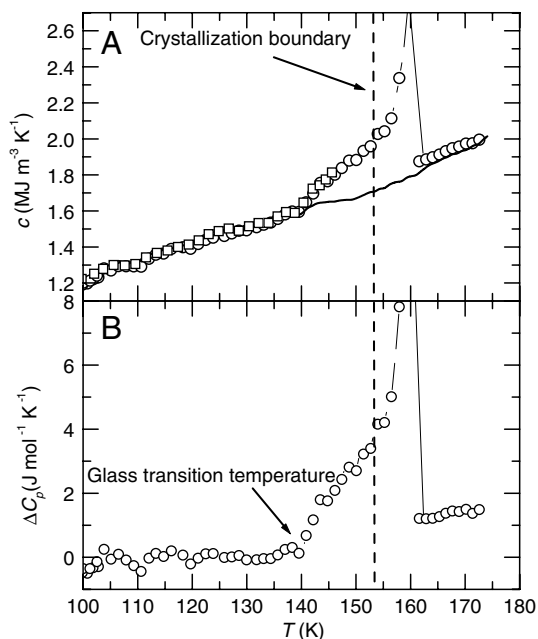


**Fig. 3.** Glass transition on heating at 1 GPa. (A) Heat capacity per unit volume of glassy water, its kinetically unfrozen state and crystallized ice (line on cooling) at 1 GPa. The squares and circles show results for two different HDA samples on heating. (In one of the runs the sample was heated only to 146 K and then cooled.) (B) Excess molar heat capacity plotted against temperature at 1 GPa. Results on heating after the sample had been pretreated by heating to 148 K at 0.4 K min<sup>-1</sup> and cooled to 100 K at 0.3 K min<sup>-1</sup>. At these heating and cooling rates, HDA slowly annealed to its ultimate high-density state, which has a  $T_g$  of approximately 140 K measured on a 1 s time scale.

intervenes at 153 K (see *SI Text*). It follows that the estimated heat capacity rise in the entire glass transition range is  $(3.7 \pm 0.4) \text{ J mol}^{-1} \text{ K}^{-1}$ , where the uncertainty of approximately 10% includes also an uncertainty in the subtracted vibrational heat capacity.

The results for HDA can be compared with those for the glass transitions of vapor-deposited amorphous solid water (ASW) (2) (see Fig. S3) and hyperquenched glassy water (HGW) (3) at 1 atm. In these cases, crystallization interferes at a temperature about 14 K above  $T_g$  and the  $C_p$  increases in this range are  $(1.9 \pm 0.2) \text{ J mol}^{-1} \text{ K}^{-1}$  (2) and  $(1.6 \pm 0.2) \text{ J mol}^{-1} \text{ K}^{-1}$  (3) for the glass-liquid transition of ASW and HGW, respectively.<sup>†</sup> (In a later study (17), a smaller value of  $0.7 \text{ J mol}^{-1} \text{ K}^{-1}$  was reported for HGW.) Thus, the heat capacity rise for HDA is larger. It is also larger than the  $C_p$  rise of  $0.7 \text{ J mol}^{-1} \text{ K}^{-1}$  (18) and  $(1.8 \pm 0.2) \text{ J mol}^{-1} \text{ K}^{-1}$  (19) at  $T_g$  of the low density amorphous ice, which forms from HDA on heating to approximately 125 K at 1 atm.

The  $C_p$  rise at 140 K shows that there is an increase of configurational degrees of freedom,<sup>‡</sup> which is normally associated with both translational and rotational diffusion. A dielectric spectroscopy study (20) has already shown the presence of reorientational motions with a relaxation time of approximately 0.3 s at 140 K (20, 21), which is in good agreement with the  $C_p$  results (see Fig. S3 and *SI Text*). In principle, the dielectric results could be due to an orientational glass transition—i.e., a transition from a state with frozen-in orientational disorder to one with reorientational motions. Haida et al. (22) have established such a transition for crystalline proton-disordered ice Ih, and it may occur in

all proton-disordered crystalline phases of ice. However, a corresponding transition here can be excluded on the basis of the amorphous structure of HDA (10, 11), and the size of the  $C_p$  increase. In the case of ice Ih (22), the  $C_p$  increase at the glass transition was small and difficult to detect even in high-accuracy adiabatic calorimetry. The  $C_p$  change observed here is larger than that for the glass to liquid transition at 1 atm, which implies that the transition cannot be associated with fewer configurational degrees of freedom than those of the glass to liquid transition. Consequently, when the glassy state at 1 GPa is heated,  $c$  indicates that the onset of structural fluctuations by diffusion on the time scale of approximately 1 s occurs at 140 K. On further heating,  $c$  of apparently ultraviscous water at 1 GPa increases rapidly as its entropy increases with increase in the structural fluctuations rate. The resulting decrease in viscosity increases the diffusion-controlled crystallization rate, and water at 1 GPa begins to crystallize at  $(153 \pm 1) \text{ K}$ . In contrast to the usual calorimetry, which shows crystallization as a local sharp minimum in the measured  $C_p$ , the technique used here shows the crystallization as a local peak in the measured  $c$  (see *SI Text*). The subsequent variation of  $c$  with temperature, shown in Fig. 3A, is typical of a completely crystallized solid.

The common behavior of easily crystallizing liquids on heating from the glassy state is structural relaxation and a glass to liquid transition followed by crystallization—i.e., the same behavior as observed here on heating of HDA at 1 GPa. Moreover, Mishima (23) has studied the nature of isothermal pressure collapse of ice Ih and found “...a smooth cross-over from (pressure induced) equilibrium melting to sluggish amorphization at around 140–165 K,” which seems consistent with the results here that HDA apparently becomes an ultraviscous liquid before crystallization at about 153 K on slow heating at 1 GPa. The results are also consistent with computer simulations that indicate a link between the annealed HDA and quenched high-pressure liquid water (24).

During the reviewing process of this work, Seidl et al. (25) have reported a study of volume expansion of HDA and suggested that HDA crystallizes before its glass transition at pressures above 0.4 GPa but shows a glass transition below 0.4 GPa. Moreover, Seidl et al. (25) discuss results to be published, which suggest a calorimetric glass transition near 115 K at 1 atm. It appears feasible that the glass transition observed here at 140 K and 1 GPa on a time scale of approximately 1 s can occur at 115 K and 1 atm on a longer time scale.

## Conclusions

Compression of ice at approximately 130 K to approximately 1.3 GPa slowly collapses it to a topologically disordered solid. On heating at 1 GPa, the structure of the solid relaxes and the relaxed state shows a glass transition with a heat capacity increase larger than for the glass to liquid transition at 1 atm. This suggests that the collapsed ice state transforms to liquid water on heating, which vitrifies on subsequent cooling or, in other words, that glassy and liquid water are connected by a reversible path under these extreme conditions. This high-density state of water is apparently favorable for suppressing crystallization, which does not occur until the relaxation time becomes less than  $10^{-2} \text{ s}$ . The relatively sluggish crystallization kinetics promotes further studies of water’s properties in its ultraviscous high-density state than is possible for the rapidly crystallizing ultraviscous liquid water at 1 atm. Moreover, because ice is one of the rock-forming minerals in the outer Solar system and most of the ice moons of Jupiter and Saturn have had some form of tectonic or internal activity, one expects that this activity would have been greatly affected by the glass transition of water with temperature change at high pressures (8). The glass transition at 1 GPa is also essential for progressing the knowledge of water’s phase diagram, which may include two liquid water phases of different densities that have a common phase coexistence line at low temperatures

<sup>†</sup> $T_g$  of water is debated, but in a review by Debenedetti (9) it was concluded that most experimental observations support  $T_g = 136 \text{ K}$  and, thus, that the  $C_p$  step at  $T_g$  of ASW and HGW are  $1.9 \text{ J mol}^{-1} \text{ K}^{-1}$  and  $1.6 \text{ J mol}^{-1} \text{ K}^{-1}$ , respectively.

<sup>‡</sup>The change in the heat capacity at  $T_g$  may also include a change in the vibrational part, but the major change is due to configurational modes.

(9). The results reported here imply the existence of at least one of these, a low-temperature high-density liquid water phase.

## Materials and Methods

Measurements were performed in situ by using the transient hot-wire method (see *SI Text* for details). Pure water (Milli-Q® Ultrapure WaterSystems) was frozen in a 14 mm deep, 39 mm internal diameter Teflon sample cell placed inside a high-pressure vessel of approximately 1.5 GPa capacity. The Teflon sample cell contained a 0.3 mm diameter and 40 mm long Ni wire (hot-wire) in the form of a circular loop that allowed simultaneous measurement of the heat capacity per unit volume,  $c$  and thermal conductivity  $\kappa$ . The hot-wire,

surrounded by the frozen water, was heated by an approximately 1 s long pulse of nominally constant power, and its electrical resistance was measured as a function of time. The wire acted as both the heater and the sensor for the temperature rise, which was calculated by using the relation between its resistance and temperature. The analytical solution for the temperature rise with time was fitted to the data points for the hot-wire temperature rise thereby yielding both  $c$  and  $\kappa$ .

**ACKNOWLEDGMENTS.** I thank G. P. Johari and H. Suga for encouraging me to look into this problem and for discussions. This work was supported financially by the Faculty of Science and Technology, Umeå University.

1. Burton EF, Oliver WF (1935) X-Ray diffraction patterns of ice. *Nature* 135:505–506.
2. Hallbrucker A, Mayer E, Johari GP (1989) Glass–liquid transition and the enthalpy of devitrification of annealed vapor-deposited amorphous solid water. A comparison with hyperquenched glassy water. *J Phys Chem* 93:4986–4990.
3. Johari GP, Hallbrucker A, Mayer E (1987) The glass–liquid transition of hyperquenched water. *Nature* 330:552–553.
4. Mishima O, Calvert LD, Whalley E (1984) “Melting” ice at 77 K and 10 kbar: A new method of making amorphous solids. *Nature* 310:393–395.
5. Koza MM, Hansen T, May RP, Schober H (2006) Link between the diversity, heterogeneity and kinetic properties of amorphous ice structures. *J Non Cryst Solids* 352:4988–4993.
6. Salzmann CG, Mayer E, Hallbrucker A (2004) Effect of heating rate and pressure on the crystallization kinetics of high-density amorphous ice on isobaric heating between 0.2 and 1.9 GPa. *Phys Chem Chem Phys* 6:5156–5165.
7. Loerting T, Salzmann C, Kohl I, Mayer E, Hallbrucker A (2001) A second distinct structural “state” of high-density amorphous ice at 77 K and 1 bar. *Phys Chem Chem Phys* 3:5355–5357.
8. Poirier JP (1982) Rheology of ices: A key to the tectonics of the ice moons of Jupiter and Saturn. *Nature* 299:683–687.
9. Debenedetti PG (2003) Supercooled and glassy water. *J Phys Condens Matter* 15: R1669–R1726.
10. Finney JL, et al. (2002) Structure of a new dense amorphous ice. *Phys Rev Lett* 89:205503.
11. Finney JL, Hallbrucker A, Kohl I, Soper AK, Bowron DT (2002) Structures of high and low density amorphous ice by neutron diffraction. *Phys Rev Lett* 88:225503.
12. Suga H, Matsuo T, Yamamuro O (1992) Thermodynamic study of ice and clathrate hydrates. *Pure Appl Chem* 64:17–26.
13. Johari GP, Andersson O (2007) Vibrational and relaxational properties of crystalline and amorphous ices. *Thermochim Acta* 461:14–43.
14. Berman R (1949) Thermal conductivity of glasses at low temperatures. *Phys Rev* 76:315–316.
15. Van Krevelen DW (1972) *Properties of Polymers* (Elsevier, Amsterdam) p 233.
16. Mishima O (1994) Reversible first-order transition between two H<sub>2</sub>O amorphs at ~0.2 GPa and ~135 K. *J Chem Phys* 100:5910–5912.
17. Kohl I, Bachmann L, Mayer E, Hallbrucker A, Loerting T (2005) Water behaviour: Glass transition in hyperquenched water? *Nature* 435:E1.
18. Handa YP, Klug DD (1988) Heat capacity and glass transition behavior of amorphous ice. *J Phys Chem* 92:3323–3325.
19. Johari GP, Hallbrucker A, Mayer E (1996) Two calorimetrically distinct states of liquid water below 150 kelvin. *Science* 273:90–92.
20. Andersson O (2005) Relaxation time of water’s high-density amorphous ice phase. *Phys Rev Lett* 95:205503.
21. Andersson O, Inaba A (2006) Dielectric properties of high-density amorphous ice under pressure. *Phys Rev B Condens Matter Mater Phys* 74:184201.
22. Haida O, Matsuo T, Suga H, Seki S (1974) Calorimetric study of the glassy state X. Enthalpy relaxation at the glass-transition temperature of hexagonal ice. *J Chem Thermodyn* 6:815–825.
23. Mishima O (1996) Relationship between melting and amorphization of ice. *Nature* 384:546–549.
24. Giovambattista N, Stanley HE, Sciortino F (2005) Relation between the high density phase and the very-high density phase of amorphous solid water. *Phys Rev Lett* 94:107803.
25. Seidl M, et al. (2011) Volumetric study consistent with a glass-to-liquid transition in amorphous ices under pressure. *Phys Rev B Condens Matter Mater Phys* 83:100201.